

X-ray diffraction and magnetic characterization of the retained austenite in a chromium alloyed high carbon steel

S. S. M. Tavares · S. R. Mello · A. M. Gomes ·
J. M. Neto · M. R. da Silva · J. M. Pardal

Received: 28 February 2005 / Accepted: 19 September 2005 / Published online: 4 May 2006
© Springer Science+Business Media, LLC 2006

Abstract In the present work the amount of retained austenite present in quenched and tempered high carbon–chromium alloyed steel was quantified by X-ray diffraction and magnetization saturation measurements. The steel was forged and directly quenched. The retained austenite partially transformed into martensite on cooling down to $-196\text{ }^{\circ}\text{C}$. The M_f temperature of about $-150\text{ }^{\circ}\text{C}$ was found by thermomagnetic analysis. Tempering at low temperatures ($220\text{ }^{\circ}\text{C}$ and $270\text{ }^{\circ}\text{C}$) promoted the stabilization effect of austenite. The intrinsic magnetization of the ferromagnetic martensite used in the phase quantification was $206.4\text{ A}^2\text{ m/kg}$. The increase of the tempering temperature above $320\text{ }^{\circ}\text{C}$ slightly decreases the m_s value of the martensite due to tempering reactions.

Introduction

High carbon martensitic steels are susceptible to austenite retention after quenching. The quantitative determination of the retained austenite is of great importance

to the steel mechanical properties. The experimental methods usually applied to quantify retained austenite include X-ray diffraction (XRD) [1], neutron diffraction (ND) [2], optical (MO) and scanning electron microscopy (SEM) [3], Mössbauer spectroscopy [3, 4], dilatometry [5] and magnetization measurements [6–8]. According to Zhao et al. [8], MO/SEM and dilatometric quantifications present low accuracy. Mössbauer and magnetization measurements present high accuracy, while XRD and ND analysis present intermediate accuracy.

In the case of magnetic quantification, the volume fraction of the ferromagnetic phase (martensite) is the ratio between the magnetic saturation of the sample analyzed by the magnetization saturation intrinsic of the magnetic phase ($m_{s(i)}$) [9]. For some applications, find the $m_{s(i)}$ of the ferromagnetic phase is the most difficult task. For instance, von Heimendahl and Thomas [10] determined the value of $160.4\text{ A}^2\text{ m/kg}$ for the α' induced by cold deformation in the austenitic stainless steel AISI 304, which was used to quantify this phase [11, 12]. Tavares et al. [13] found the value of $133\text{ A}^2\text{ m/kg}$ for the ferrite phase in the duplex stainless steel UNS S31803 (2205). The intrinsic magnetization saturation of the ferromagnetic phase generally depends on its chemical composition. The quantification by magnetization measurements is only possible if the magnetization saturation of the ferromagnetic phase $m_{s(i)}$ do not change significantly with the phase proportions.

In the present paper, the retained austenite of quenched and tempered high carbon chromium alloyed steel for balls used in ore mining industries was quantified by XRD and magnetic measurements. The effect of tempering temperature and subzero cooling on the austenite volume fraction were evaluated.

S. S. M. Tavares (✉) · S. R. Mello · J. M. Pardal
Departamento de Engenharia Mecânica-PGMEC, Universidade
Federal Fluminense, Rua Passo da Pátria, 156, CEP 24210-240
Niterói, Rio de Janeiro, Brazil
e-mail: ssmtavares@terra.com.br

A. M. Gomes · J. M. Neto
Instituto de Física, Universidade Federal do Rio de Janeiro,
Rio de Janeiro, Brazil

M. R. da Silva
UNIFEI, Itajubá, Brazil

Experimental

Samples of a high carbon chromium alloyed steel (composition shown in Table 1) were forged between 1120 °C (start) and 950 °C (finish) and then air cooled to one of the quenching temperatures: 880 °C, 810 °C or 750 °C. The prior austenite grain size of the different samples was the same, since they were austenitized at the same temperature (1120 °C) and forged with the same deformation. Quenching was performed in a polymer plus water solution at 50–60 °C. The samples quenched from 810 °C were tempered in the 220–600 °C range. The samples quenched from 750 °C and 880 °C were only tempered at 220 °C. Table 2 shows the samples identifications used in this work. The samples identified with the letter ‘‘N’’ were dipped in liquid nitrogen (–196 °C) before the phase quantification.

Magnetic measurements were performed in a Vibrating Sample Magnetometer (VSM) at room temperature with maximum applied field of 800 kA/m, time constant of 1 ms and total measuring time of 10 min. Magnetization saturation values of all samples were obtained from the hysteresis loops. The samples A1, B1, C1, C3 and C5 were measured in the VSM, immersed in the liquid nitrogen (–196 °C) and measured again. Thermomagnetic analysis from 25 °C to –196 °C were carried out in a Physical Properties Measurement System with scanning rate of 5 °C/min.

Metallographic specimens for optical microscopy were prepared by the usual grinding and polishing procedure. The samples were etched with nital 2%.

The XRD measurements were carried out using a powder diffractometer PHILIPS®, model X’Pert Pro, in step scan mode with step size of 0.02°, time per step 3 s and 2θ angular interval of 45°–105°. It was used CoK_α (1.7890 Å) radiation with 40 kV and 40 mA.

The volume fraction of the austenite (γ) and martensite (α) phases were obtained by the direct comparison method, using the following equations [14]:

$$\frac{I_\alpha}{I_\gamma} = \frac{K_\alpha C_\alpha}{K_\gamma C_\gamma} \tag{1}$$

$$K_{\alpha,\gamma} = \frac{1}{v^2} \left[|F|^2 m \left(\frac{1 + \cos^2 \theta}{\sin^2 \theta \cos \theta} \right) \right] \left(\frac{e^{-2M}}{2\mu} \right) \tag{2}$$

$$C_\alpha + C_\gamma = 1 \tag{3}$$

where *v* is the unit cell volume of each phase, *F* is the structure factor, *m* is the multiplicity factor, *θ* is the reflection angle of the peak analyzed, *e*^{–2*M*} is the Debye–Waller factor and *μ* is absorption coefficient of each phase. The diffraction peaks corresponding to the planes of each phase were compared all against all. The average value of all the compared diffraction peaks was calculated to minimize the preferential direction effect. The analyzed peaks were: (111)_A, (110)_M, (200)_A, (200)_M, (220)_A, (211)_M, (311)_A, (222)_A, and (220)_M, except for the sample B1, where the reflection (222)_γ was not present.

Results and discussion

Figure 1a and b show retained austenite islands in the samples quenched and tempered at 220 °C.

Figure 2 shows the X-ray diffractograms of the samples A1, B1 and C1, which were tempered at 220 °C after quenching from 750 °C, 880 °C and 810 °C, respectively. Figure 3 compares the diffractograms of the samples quenched from 810 °C and tempered at 220 °C (C1), 270 °C (C3) and 320 °C (C5). This figure confirms that the amount of retained austenite decreases with the increase of tempering temperature and shows that the sample tempered 320 °C did not present any diffraction peak of austenite.

Figures 4 and 5 show the thermomagnetic analysis curves of samples B1 and C1, respectively. Although the estimated *M_s* temperature of the steel is about 115 °C, the austenite of sample B1 starts to transform upon cooling only at –15 °C. This is one of the features of the stabilization of the austenite described by Verhoeven [15]. If the γ → M transformation is interrupted in some point between *M_s* and *M_f* resting a large period of time at this temperature, the re-starting of the transformation upon cooling will be retarded. In sample C1 some stabilization also occurs, since transformation is more intense only below –13 °C.

The γ → M transformation finishes at –150 °C and –140 °C in samples B1 and C1, respectively. However, Fig. 6 shows that the sample C1N, which was cooled to –196 °C, still presents considerable amounts of

Table 1 Chemical composition of the steel

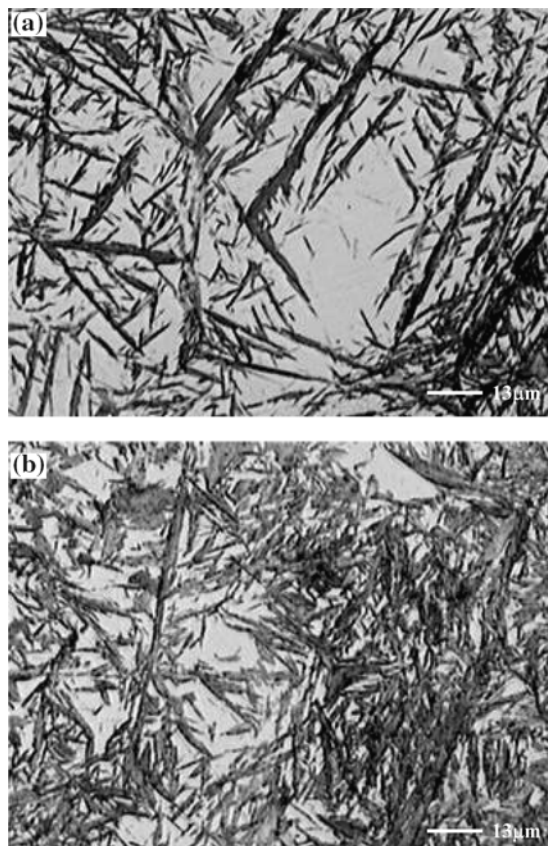
%C	%Si	%Mn	%S	%P	%Cr	%Nb	%Mo
0.93	0.21	0.69	0.004	0.013	0.68	0.032	0.140

Table 2 Identification of the samples produced

Quenching temperature (°C)	Tempering temperature (°C)	Samples identification
750 °C	220	A1/A1N
880 °C	220	B1/B1N
810 °C	220	C1/C1N
	270	C3/C3N
	320	C5/C5N
	400	C7
	450	C9
	500	C11
	550	C13
	600	C15

retained austenite. This is another feature of the austenite stabilization [15]. After some hours at room temperature and tempering at 220 °C the amount of retained austenite transformed upon subzero cooling is decreased.

Figure 7 shows the magnetization curves of the samples C1, C3 and C5. Figure 8 shows the magnetization saturation versus tempering temperature behavior of the samples quenched from 810 °C. The increase of the magnetization saturation with dip cooling into liquid nitrogen is due to the partial transformation of retained austenite. The results of Fig. 8 suggest that the increase of the tempering temperature from 220 °C to 270 °C enhances the austenite

**Fig. 1** Microstructures of samples B1(a) and C1(b)

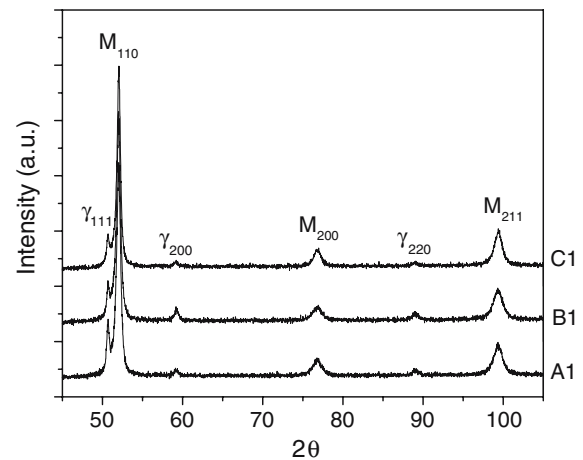
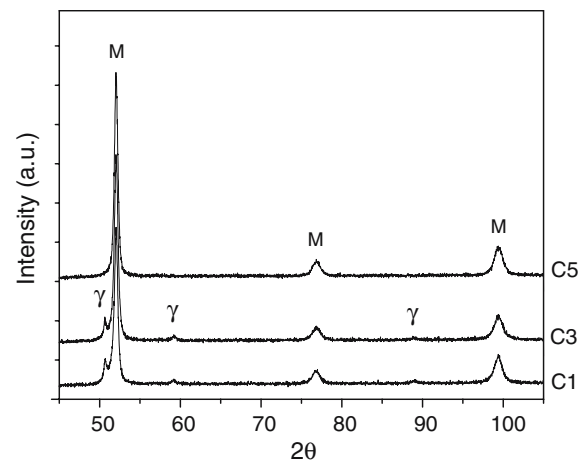
stabilization effect. The cooling to liquid nitrogen converts about 63% of the austenite present in the sample tempered at 220 °C (compare C1 and C1N results), while only 14% of the austenite present in the sample tempered at 270 °C is converted by subzero cooling.

The sample tempered at 320 °C (C5) presents a very little amount of retained austenite in the microstructure, undetectable by XRD (Fig. 3). Samples tempered at 400 °C or higher do not present austenite in the microstructure.

The m_s value of 206.4 A m²/kg of the sample C5N (quenched from 810 °C, tempered at 320 °C and dip cooled into liquid nitrogen) was used to quantify the amounts of martensite and austenite of the samples quenched and tempered at 220 °C, 270 °C and 320 °C using the equations:

$$C_M = \frac{m_s(\text{A m}^2/\text{kg})}{206.4(\text{A m}^2/\text{kg})} \quad (4)$$

$$C_\gamma = 1 - C_M \quad (5)$$

**Fig. 2** Diffractograms of samples A1, B1 and C1**Fig. 3** Diffractograms of samples C1, C3 and C5

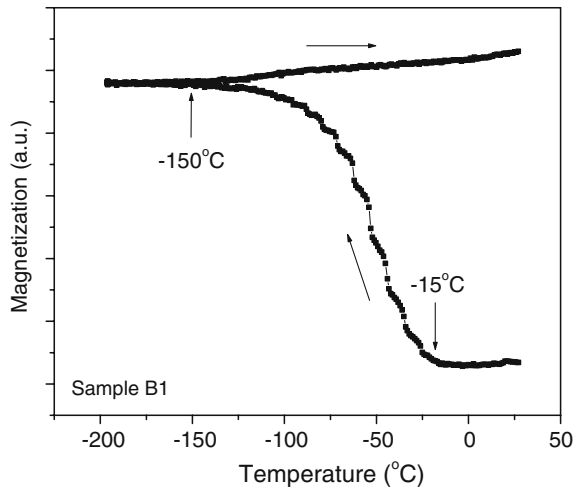


Fig. 4 TMA curve of sample B1

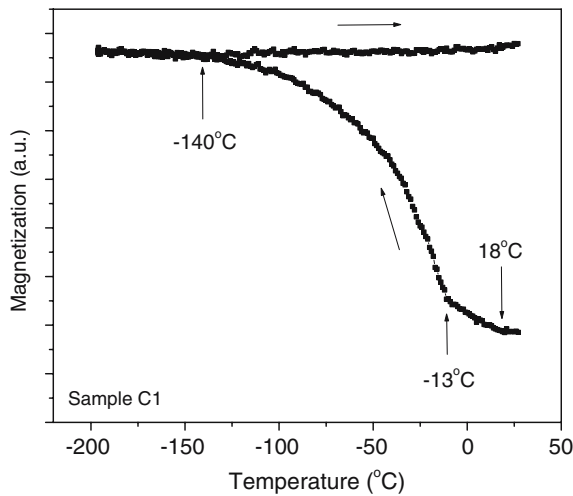


Fig. 5 TMA curve of sample C1

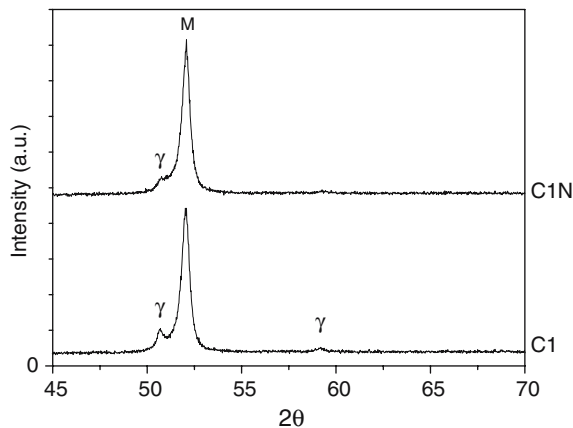


Fig. 6 X-ray diffractograms of samples C1 and C1N

where m_s is the saturation magnetization of the analyzed sample. The value of $206.4 \text{ A m}^2/\text{kg}$ was taken as the $m_{s(i)}$ value of the martensite phase, considering that the martensite matrix of samples tempered at temperatures lower than $320 \text{ }^\circ\text{C}$ all present similar compositions and, hence, the same $m_{s(i)}$ value.

It is worth noting that the behavior shown in Fig. 8 is the opposite of the observed in a high 13%Cr martensitic stainless steel AISI 420 [16] where the tempering reactions lead to an increase of m_s . In that case, the matrix became more ferromagnetic due to the chromium carbide precipitation which promotes the depletion of chromium in the matrix. The result was the increase of m_s because the dissolved chromium decreases the magnetic moment of iron. In the present case, the tempering above $320 \text{ }^\circ\text{C}$ promotes the precipitation of increasing amounts of Fe_3C , which is less ferromagnetic than the martensitic matrix. Although the reduction of the amount of solid solution carbon of the martensitic matrix also tends to increase the magnetic moment of iron, the overall behavior is the decrease of the m_s of the alloy.

Table 3 shows the results of austenite volume fraction quantifications by XRD and magnetization saturation measurements. For both methods the austenite volume fraction (C_γ) was higher in the sample quenched from the highest temperature ($880 \text{ }^\circ\text{C}$). It is interesting to note that the quantification by XRD provide results 0.06–0.07 lower than the magnetization measurements in samples A1, B1 and C1. However, in samples where the austenite was partially transformed by subzero cooling (C1N) or tempering at $270 \text{ }^\circ\text{C}$ the quantification by XRD gives results 0.3–0.4 higher than the magnetization measurements ones.

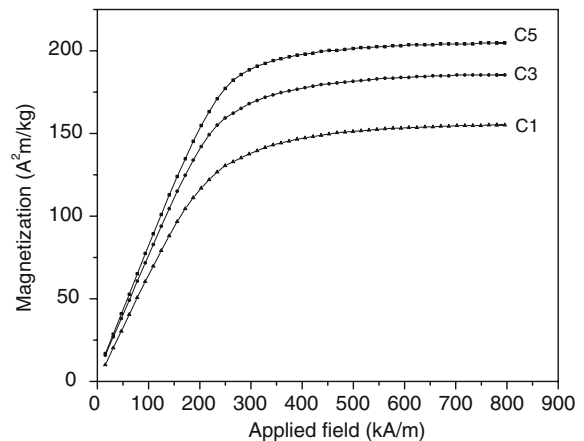


Fig. 7 Magnetization curves of samples C1, C3 and C5

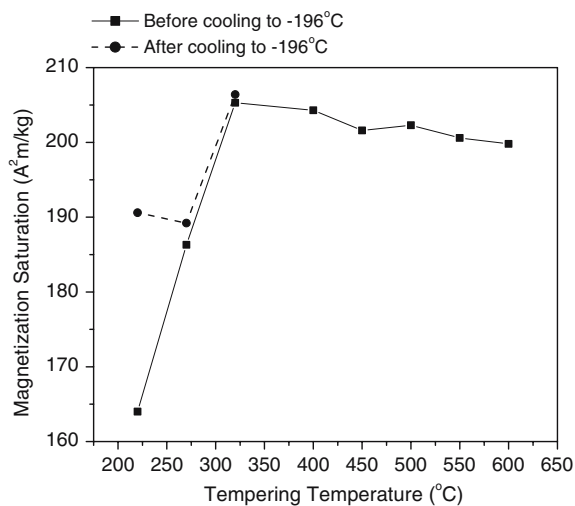


Fig. 8 Magnetization saturation against tempering temperature

Table 3 Results of phase quantifications by XRD and magnetization saturation measurements

Quenching temperature (°C)	Tempering temperature (°C)	Sample identification	Austenite volume fraction (C_7)	
			XRD	Magnetic method
750	220	A1	0.162	0.219
		A1N	–	0.097
880	220	B1	0.202	0.275
		B1N	–	0.089
810	220	C1	0.138	0.205
		C1N	0.112	0.076
	270	C3	0.128	0.097
		C3N	–	0.083
	320	C5	0.0	0.005
		C5N	–	0.0
400	C7	0.0	0.0	

Conclusions

Quantifications of the retained austenite in quenched and tempered high carbon chromium alloyed steel were performed by XRD and magnetic measurements. The samples quenched from 880 °C, 810 °C and 750 °C presented austenite volume fractions ranging from 0.275 to 0.205 by the magnetic method and from 0.138 to 0.202 by the XRD

analysis. The retained austenite transforms partially into martensite upon cooling down to -150 °C. Some of the retained austenite remains untransformed due to the stabilization of the austenite. The increase of the tempering temperature from 220 °C to 270 °C decreases the austenite amount but enhances the stabilization effect of the austenite to subsequent cooling. The intrinsic magnetization of the ferromagnetic martensite adopted in this work in the phase quantifications was 206.4 A^2m/kg . The increase of the tempering temperature above 320 °C slightly decreases the m_s value. The sample tempered at 320 °C presented a very small amount of retained austenite ($<1\%$), only detectable by the magnetic saturation method.

Acknowledgements The authors acknowledge of the Brazilian research agencies (CAPES, FAPERJ and CNPq) for financial support.

References

1. Leem DS, Lee YD, Jun JH, Choi CS (2001) Scripta Materialia 45:767
2. Bouet M, Root J, Es-Sadiki E (1998) Mater Sci Forum 284–286:319
3. Jacques P, Cornet X, Harlet Ph, Ladrière J, Delannay F (1998) Metall Trans 29A:2383
4. Ladrière JH, He XJ, (1986) Mater Sci Eng 77:133
5. Ali A, Ahmed M, Hashimi FH, Khan AQ (1993) Metall Trans 24A:2145
6. Bleck W, Hulka K, Papamentellos K (1998) Mater Sci Forum 284–286:327
7. Gladkovskii SV, Kaletina YuV, Filippov AM, Kaletin AY, Schastlivtsev VM, Ishina EA, Veselov IN (1999) The Ph Met Metall 87(3):253
8. Zhao L, van Dijk NH, Brück E, Sietsma J, van der Zwaag S (2002) Mater Sci Eng A313:145
9. Cullity BD (1992) Introduction to magnetic materials. Addison-Wesley Publishing Company, Massachusetts - USA
10. von Heimendahl M., Thomas G. (1964) Trans TMS-AIME 230:1520
11. Mangonon PL, Thomas G (1970) Metall Trans 1:1587
12. Tavares SSM, Miraglia S, Fruchart D (2000) J Alloys Compounds 307:311
13. Tavares SSM, Neto JM, da Silva MR, Pedroza PD, Teodósio JR, Pairs S (2003) J Alloys Compounds 351(1–2):283
14. Cullity BD (1956) Elements of X-ray diffraction. Addison-Wesley Publishing Company, Massachusetts – USA, 514 pp
15. Verhoeven JD (1975) Fundamentals of physical metallurgy. Iowa, USA, pp 457–511
16. Tavares SSM, Laborie D, Miraglia S, Fruchart D (2000) J Alloys Compounds 32:307